

## Electron-electron scattering in simple metals

Carl A. Kukkonen

*Department of Physics, Cornell University, Ithaca, New York 14853  
and Research Staff,\* Ford Motor Company, Dearborn, Michigan 48121*

John W. Wilkins

*Laboratory of Atomic and Solid State Physics and Materials Science Center, Cornell University, Ithaca, New York 14853*

(Received 14 December 1978)

The interaction between two-electron quasiparticles is approximated in terms of the dielectric and vertex functions of the uniform electron gas. These functions must satisfy the compressibility sum rule, and this fact makes the interaction at metallic densities much stronger than the Thomas-Fermi screened Coulomb interaction. A problem arises in applying this theory to real metals because the compressibility of the electron gas at densities appropriate to rubidium and cesium is negative. This anomaly is removed by taking into account the real metal effect of core polarization. The effective interaction is used to calculate the electron-electron scattering rate and its contribution to the thermal resistivity. The result is consistent with the single experimental measurement presently available on sodium (new results on potassium, rubidium, and cesium became available after this paper was completed; these are reported in Table III), whereas the Thomas-Fermi interaction predicts a thermal resistivity that is too small by a factor of 7. The scattering rates and thermal resistivities of all the alkali metals are calculated to enable comparison with future experimental values.

### I. INTERACTION

This work was motivated by the experiments of Cook, Van der Meer, and Laubitz<sup>1</sup> who carefully measured both the electrical and thermal resistivities of sodium from 40 to 360 K and used an ingenious method<sup>2</sup> to extract from their data the contribution of electron-electron scattering to the thermal resistivity. Kukkonen and Smith<sup>3</sup> calculated this quantity using the Thomas-Fermi screened Coulomb interaction and obtained a result that was *smaller* than experiment by a factor of 7. One aim of this paper is to resolve this discrepancy.

This paper is organized as follows. In Sec. II we obtain an approximate electron-electron interaction  $U_{ee}(q)$  in terms of  $\epsilon(q)$  and  $\Lambda(k_F, q)$ , the dielectric and vertex functions and  $z(k_F)$ , the quasiparticle renormalization factor, of the uniform electron gas,

$$U_{ee} = z^2(k_F) \Lambda^2(k_F, q) \frac{V(q)}{\epsilon(q)}, \quad (1)$$

where  $V(q) = 4\pi e^2/q^2$ . This interaction is appropriate for electrons with opposite spins. The vertex function takes into account the Pauli principle in that the screening cloud around an electron is due both to its charge and to the Pauli principle. Since we are discussing the interaction of two-electron quasiparticles, there is a vertex function associated with each of them. [We note that the Thomas-Fermi interaction considers both  $z(k_F)$  and  $\Lambda(k_F, q)$  to be unity.] We make no attempt to

do an independent calculation of the dielectric and vertex functions; rather, we examine and test the consequences of several existing calculations.

There are constraints on the model interaction [Eq. (1)] because the  $q=0$  limits of both the dielectric and vertex functions are exactly related to the compressibility of the electron gas. Requiring that the compressibility obtained from the ground-state energy is identical to that obtained from an appropriate  $q=0$  limit of the dielectric function is called the compressibility sum rule.

The dielectric functions of Hubbard<sup>4</sup> (as modified by Geldart and Vosko<sup>5</sup>) and of Geldart and Taylor<sup>6</sup> include an adjustable parameter which is determined by satisfying the compressibility sum rule. Vashishta and Singwi<sup>7</sup> have used a self-consistency technique to obtain a dielectric function that also satisfies the sum rule. Because Geldart and Taylor and Vashishta and Singwi do not calculate the vertex function, we propose a method for extracting it from the dielectric function which allows us to form the effective electron-electron interaction.

The interactions determined by these three dielectric functions agree at  $q=0$  because of the sum rule, and they also agree at large  $q$ . For intermediate  $q$  they are different, and we examine the two extremes—the Hubbard and the Geldart and Taylor interactions—in detail.

The constraint imposed by the compressibility sum rule turns out to be extremely important, but it also presents an immediate problem when we try to apply it to real metals. This is because the compressibility of the uniform electron gas be-

comes negative for  $r_s > 5.18$ . Since rubidium at  $r_s = 5.20$  and cesium at  $r_s = 5.63$  lie in this region, we are led to examine the physics of a real metal more closely. The details of this examination are in Sec. III.

In a metal there is an additional contribution to the dielectric function due to the polarization of core electrons in the periodic lattice of ions. Taking the core polarizability to be a constant, we view the ionic background as a uniform, charged, and polarizable medium in which the electrons move. In order to generalize the effective interaction to include the effects of core polarization, we must find the dielectric and vertex functions of the combined system of the electron gas and the polarizable background. The Hamiltonian of an electron gas with mass  $m_B$  immersed in a polarizable background of dielectric constant  $\epsilon_B$  may be written in exactly the same form as the Hamiltonian of an electron gas without a polarizable background, except that the charge  $e^2$  is replaced by  $e^2/\epsilon_B$ . We show in Appendix A by a scaling or homogeneity argument that the dielectric function of this model system at a density determined by  $r_s$  can be expressed in terms of the known dielectric function of the electron gas with  $\epsilon_B = 1$ , but at a new density determined by  $m_B r_s / m \epsilon_B$ .

The most important consequence of including core polarization is to modify the compressibility sum rule so that, in addition to reducing the strength of the effective interaction, the criterion for a positive compressibility becomes  $m_B r_s / m \epsilon_B < 5.18$  rather than  $r_s < 5.18$ . Using semiempirical values for  $\epsilon_B$  we find that both rubidium and cesium are renormalized into the region of *positive* compressibility.

With these results we are prepared to numerically evaluate the effective interaction and the electron-electron scattering contribution to the thermal resistivity. This is done in Sec. IV, where we exhibit and compare  $U_{ee}(q)$  and  $U_{ee}(r)$  calculated using the Hubbard and Geldart and Taylor dielectric functions with the simple Thomas-Fermi screened Coulomb interaction. We find that because of the constraints imposed by the compressibility sum rule the Hubbard and Geldart and Taylor effective interactions are considerably stronger than the Thomas-Fermi result. Motivated by the simplicity of the Thomas-Fermi interaction, we write an interpolation formula for the effective interaction which has the Thomas-Fermi form, but with a new screening wave vector defined so that the compressibility sum rule is satisfied. This interpolation formula is a close approximation to the more complicated Hubbard result.

The thermal resistivities calculated using the Hubbard and Geldart and Taylor interactions are

much larger than those predicted by Thomas-Fermi theory, and both predictions are within the experimental error of the measurement on sodium. Summarizing the results for sodium, we find that (in units of  $10^{-6}$  cm/W)

$$\begin{aligned} W_{e1}/T &= 20 \text{ (Thomas-Fermi)} \\ &= 95 \text{ (Geldart and Taylor)} \\ &= 130 \text{ (Hubbard)} \\ &= 140 \pm 70 \text{ (experiment}^1) \end{aligned}$$

and we expect that the Vashishta-Singwi result would fall between those of Hubbard and Geldart and Taylor. We calculate the thermal resistivities and scattering rates for all the alkali metals to enable comparison with future experiments. The predicted resistivities of potassium, rubidium, and cesium are sensitive functions of the dielectric constant of the background. For example, the resistivity of potassium is reduced by more than a factor of 3 when  $\epsilon_B$  is changed from 1 to 1.14. This change is sufficiently dramatic that experiments on these metals should be able to determine if our treatment of the polarizable background is adequate.

The point we wish to emphasize most is the importance of the compressibility sum rule. Since the effective interaction between two electrons depends strongly on the vertex and dielectric functions, which must satisfy the sum rule, this sum rule is of paramount importance, and dielectric functions which deviate significantly from it cannot be used to construct the effective interaction.

In Appendix B we examine the four-point scattering function and show how the form of the effective interaction [Eq. (1)] may be motivated. We also examine the Bethe-Salpeter equation for the four-point function and note the limitations of the phase-shift approximation of the electron-electron scattering rate.

## II. THE INTERACTION

### A. Approximate electron-electron interaction

There are three basic screened Coulomb interactions in a metal: (i) the effective interaction between two external "test" charges, e.g., the screened ion-ion interaction used to calculate phonon frequencies in simple metals, (ii) the interaction between an electron and a test charge, which is needed to calculate the scattering of an electron by an ionized impurity, and (iii) the effective interaction between two electrons. We define the effective interaction as the Born approximation of the total scattering amplitude. The first two of these effective interactions have been widely

investigated. We will discuss these two only briefly to define our notation and to show how the electron-electron interaction differs from them.

Simple calculations of the effective interaction take into account the Coulomb interaction between the charge under consideration (e.g., test charge or electron) and the screening electrons, but neglect the interaction of the screening electrons with each other. In this approximation, all three effective interactions are identical and in Thomas-Fermi theory are equal to

$$U_{\text{TF}}(q) = 4\pi e^2 / (q^2 + q_{\text{TF}}^2), \quad (2)$$

where  $q_{\text{TF}}$  is the magnitude of the screening wave vector. A more sophisticated approach, the Lindhard<sup>8</sup> or the random-phase approximation, yields the effective interaction that is the bare Coulomb interaction,  $V(q) = 4\pi e^2 / q^2$ , screened by the Lindhard dielectric function,  $\epsilon_L(q)$ . This interaction is equal to  $U_{\text{TF}}(q)$  at  $q = 0$ .

When electron-electron interactions are included, these three effective interactions differ. The test-charge-test-charge interaction,  $U_{\text{tt}}(q)$ , is modified because the screening electrons now avoid each other due to the Pauli principle (exchange) and due to their mutual Coulomb repulsion (correlation). This interaction may be formally written

$$U_{\text{tt}}(q) = V(q) / \epsilon(q), \quad (3)$$

where  $\epsilon(q)$  is the exact but largely unknown dielectric function of the electron gas.

The electron-test-charge interaction,  $U_{\text{et}}(q)$  differs from  $U_{\text{tt}}(q)$  because the electron under consideration is indistinguishable from the screening electrons, and therefore it has an exchange as well as a direct Coulomb interaction with them. A formally exact solution of this problem has also been obtained. The effective interaction between an electron on the Fermi surface ( $|\vec{k}| = k_F$ ) and a test charge is given by<sup>9,10</sup>

$$U_{\text{et}}(q) = z(k_F) \Lambda(k_F, q) V(q) / \epsilon(q). \quad (4)$$

Note that  $U_{\text{et}}(q) = z(k_F) \Lambda(k_F, q) U_{\text{tt}}(q)$ . Therefore the vertex function represents the exchange modification of the interaction when an electron is substituted for a test charge.

The problem of concern in this paper is the effective electron-electron interaction,  $U_{\text{ee}}(q)$ . This case is more complicated than those discussed above because now both electrons under consideration may exchange with the screening electrons. Furthermore, if they have parallel spins they may exchange with each other as well. Because of these complications, there is no simple formal result for  $U_{\text{ee}}(q)$  and the problem must be

addressed through the Bethe-Salpeter equation (see Appendix B).

We propose a simple approximate electron-electron interaction that is a natural extension of the electron-test-charge interaction. We assume that the two electrons under consideration (with opposite spins) exchange with the screening electrons independently. Therefore each electron acquires a vertex correction and the approximate effective interaction between electrons with opposite spins is given by

$$U_{\text{e}^{\uparrow}\text{e}^{\downarrow}}(q) = [z(k_F) \Lambda(k_F, q)]^2 V(q) / \epsilon(q). \quad (5)$$

Since this approximation treats the two electrons as independent quasiparticles, the interaction between two electrons with parallel spins is formed in the usual way,

$$U_{\text{e}^{\uparrow}\text{e}^{\uparrow}}(q) = U_{\text{e}^{\uparrow}\text{e}^{\downarrow}}(q) - U_{\text{e}^{\uparrow}\text{e}^{\downarrow}}(k_2 - k_1 - q), \quad (6)$$

where  $\vec{k}_1$  and  $\vec{k}_2$  are the initial momenta of the two electrons under consideration. In Appendix B, we consider the Bethe-Salpeter equation and show that Eqs. (5) and (6) are a reasonable first approximation to the effective electron-electron interaction.

With these results, we have formal expressions for all three interactions in a metal written in terms of the dielectric and vertex functions of the electron gas. Unfortunately, these functions are not precisely known. We do not make an independent calculation of these functions, but use several existing dielectric functions and extract the vertex function from  $\epsilon(q)$  by the procedure discussed below. Kleinman<sup>11</sup> has also discussed these three interactions and their formal relationships.

#### B. Constraints on the model interaction

The static dielectric function is defined in terms of the proper polarization,  $\Pi(q)$ , as<sup>5,12</sup>

$$\epsilon(q) = 1 + V(q) \Pi(q). \quad (7)$$

There exists an exact relation between the proper polarization and the compressibility  $\kappa$  which is given by<sup>5</sup>

$$\frac{\Pi(q=0)}{\Pi^0(q=0)} = \frac{\kappa}{\kappa_0}, \quad (8)$$

where  $\Pi^0(q)$  is the polarization and  $\kappa_0$  is the compressibility of a system of noninteracting electrons. This relation is due to a Ward identity<sup>5,13-17</sup> and is known as the compressibility sum rule. Note that  $\kappa$  is the compressibility of the electron gas alone. It is not the measured compressibility of the metal. Another Ward identity yields the exact result that<sup>13-17</sup>

$$\Lambda(k_F, q=0) = \frac{1}{(m^*/m)z(k_F)} \frac{\kappa}{\kappa_0}, \quad (9)$$

where  $m^*$  is the effective mass due to electron-electron interactions. Explicit calculations of the effective mass show it to be approximately equal to the bare mass in simple metals<sup>18</sup>; hence we take  $m^*/m=1$ .

These two exact relations, together with the physical requirement that for large  $q$ ,  $U_{\text{ee}}(q)$  goes to  $4\pi e^2/q^2$ , are the only *a priori* criteria we have to judge the effective interaction and as we shall see, they have a profound effect on the strength of the interaction.

### C. Compressibility

In order to use the Ward identity and the compressibility sum rule, we need to know the compressibility of the uniform electron gas.

The compressibility is determined by the second derivative of the total energy with respect to the volume,

$$\kappa = \left( V \frac{\partial^2 E}{\partial V^2} \right)^{-1}. \quad (10)$$

There are many different calculations of the ground-state energy of the electron gas and their internal agreement is quite good. Furthermore, since the compressibilities determined by the most recent calculations also agree quite well with each other,<sup>7</sup> it is commonly accepted<sup>5,19</sup> that they yield something close to the true compressibility. In our calculations we use the compressibility determined from the energy calculation of Vashishta and Singwi<sup>7,20</sup>:

$$\frac{\kappa_0}{\kappa} = 1 - \frac{\alpha r_s}{\pi} \left[ 1 + \frac{0.0335\pi\alpha r_s}{2} + \frac{0.02\pi\alpha r_s^2}{3} \left( \frac{0.1 + 2r_s}{(0.1 + r_s)^3} \right) \right], \quad (11)$$

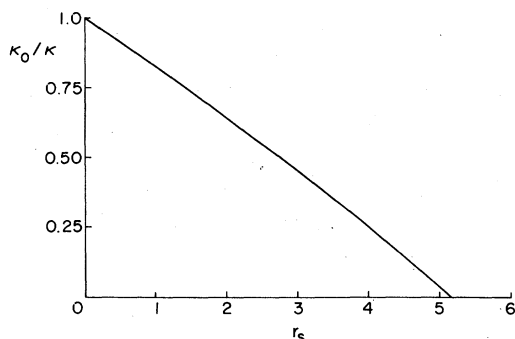


FIG. 1. Ratio of the free-electron compressibility to the compressibility of interacting electron gas as a function of  $r_s$ .  $\kappa$  was obtained by differentiating the ground-state energy of Vashishta and Singwi.

where  $\alpha = (4/9\pi)^{1/3} = 0.52106$  and the particle density is given by  $n^{-1} = V/N = \frac{4}{3}\pi(r_s a_0)^3$ , and  $a_0$  is the Bohr radius (0.529 Å). This expression is plotted in Fig. 1.

We note that the compressibility ratio becomes negative for  $r_s > 5.18$ . This is due to a divergence in  $\kappa$ . The divergence occurs at  $r_s = 6.03$  in Hartree-Fock theory. Including the correlation energy moves the divergence to smaller  $r_s$ . Since rubidium at  $r_s = 5.20$  and cesium at  $r_s = 5.63$  lie in the region of negative compressibility, we will need to examine other aspects of the physics of alkali metals more closely. We do this in Sec. III.

### D. Approximations for the dielectric and vertex functions

The simplest approximation for  $\pi(q)$  was calculated by Lindhard<sup>8</sup> in 1954. His result, designated by  $\pi^0(q)$ , assumes noninteracting electrons and is equivalent to the random-phase approximation. The expression for  $\pi^0(q)$  is

$$\Pi^0(q) = \frac{q_{\text{TF}}^2}{4\pi e^2} \left( \frac{1}{2} + \frac{k_F}{2q} [1 - (q/2k_F)^2] \ln \left| \frac{1 + q/2k_F}{1 - q/2k_F} \right| \right). \quad (12)$$

In this approximation, the vertex function is unity and all three effective interactions are equal. Since the Lindhard dielectric function does not satisfy the compressibility sum rule, it cannot be used to form  $U_{\text{ee}}(q)$ . The Lindhard interaction is equal to  $U_{\text{TF}}(q)$  at  $q=0$  and for finite  $q$  the discrepancy is small and it has been shown that  $U_{\text{TF}}(q)$  predicts a thermal resistivity much smaller than observed.

The most widely used improvement of Lindhard's result, due to Hubbard,<sup>4</sup> includes the effect of exchange in an appropriate way. In the Hubbard approximation the proper polarization is given by<sup>5,19</sup>

$$\Pi(q) = \Lambda(q)\Pi^0(q), \quad (13)$$

where

$$\Lambda^{-1}(q) = 1 - (1 - \kappa_0/\kappa) \left( \frac{q_{\text{TF}}^2}{q_{\text{TF}}^2 + 2q^2(1 - \kappa_0/\kappa)} \right) \frac{\Pi^0(q)}{\Pi^0(0)}. \quad (14)$$

Hubbard's original form for  $\Pi(q)$  did not satisfy the compressibility sum rule and the expression given above, which incorporates the sum rule, is an improvement due to Geldart and Vosko.<sup>5</sup> Henceforth when we use the term Hubbard approximation we will mean as modified by Geldart and Vosko. The precise interpretation of  $\Lambda(q)$  is a source of some possible confusion; the small  $q$  limit of  $\Lambda(q)$  is  $\kappa/\kappa_0$ , whereas the proper vertex function must approach  $[1/z(k_F)]\kappa/\kappa_0$  by the Ward

identity [Eq. (9)]. Therefore the identification

$$z(k_F)\Lambda(k_F, q) = \Lambda(q) = \Pi(q)/\Pi^0(q) \quad (15)$$

is exact in the small  $q$  limit. We assume it to be true for all  $q$ . Hedin and Lundqvist<sup>19</sup> point out that the large  $q$  limit of  $\Lambda(k_F, q)$  is unity and not  $1/z(k_F)$ , so that this identification is wrong for large  $q$ . However, the following discussion will show that the error introduced by using Eq. (15) for all  $q$  is small when calculating the thermal resistivity.

Equation (15) is exact for small  $q$ , but its use predicts an interaction that is equal to the bare interaction  $V(q)$  for large  $q$  where the correct large  $q$  limit is  $U_{ee}(q) = z^2(k_F)V(q)$ . For our application to electron-electron scattering  $q$  can be at most  $2k_F$  and the importance of the renormalization factor at this momentum transfer is not known. We can, however, estimate this effect by assuming that the effective interaction is

$$[(1 - q/2k_F) + (q/2k_F)z^2(k_F)]$$

times the interaction obtained by using Eq. (15). This interpolation assumes that the effect of  $z(k_F)$  turns on smoothly with  $q$  and reaches its full large limit by  $q = 2k_F$ . We have estimated that thermal resistivities calculated with this interpolated interaction using  $z(k_F) \sim 0.7$ <sup>12</sup> will be only a few percent smaller than those calculated using the as-

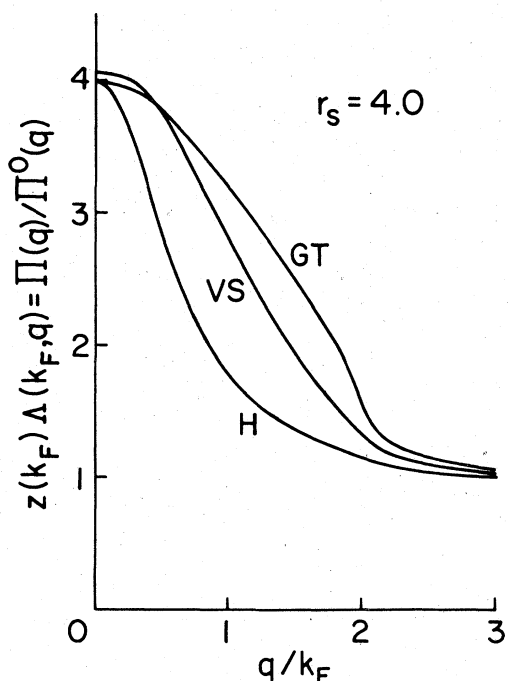


FIG. 2. Plot of  $z(k_F)$  times the vertex function vs  $q$  for the Hubbard (H), Vashishta and Singwi (VS), and Geldart and Taylor (GT) approximations at  $r_s = 4.0$  [Eq. (15)].

sumption of Eq. (15), and thus this assumption is well justified. Calculations of other properties that depend more strongly on large  $q$  may require more care. With this approximation for the vertex function, the effective electron-electron interaction is completely specified within the Hubbard approximation.

The main thrust of most recent investigators<sup>7,11,21,22</sup> has been directed toward calculating  $\epsilon(q)$  by variational or self-consistency techniques. Unlike the Hubbard approximation which includes a free parameter that is determined by satisfying the compressibility sum rule, these schemes have no adjustable constants. Vashishta and Singwi<sup>7</sup> have succeeded in obtaining a dielectric function that agrees well with the compressibility determined by their energy calculation.

Another approach was taken by Geldart and Taylor,<sup>6</sup> who used the integral equation formalism of many-body theory to compute directly, but approximately, the proper polarization. In their estimate of the effect of higher-order processes, they include an adjustable parameter which is determined by satisfying the compressibility sum rule. Geldart and Taylor assert that their work includes exchange and correlation in a self-consistent manner, and state that their  $\Pi(q)$  is quite different from that of the Hubbard approximation as may be seen in Fig. 2.<sup>23</sup> Their version of the proper polarization is given in tabular form for various values of  $r_s$ .

The only dielectric functions that satisfy the compressibility sum rule<sup>21</sup> are those of Hubbard, Vashishta, and Singwi (within a few percent), and Geldart and Taylor. The last two do not calculate the vertex function; however, we assume that it can be obtained from the proper polarization by the prescription of Eq. (15). With this assumption we can form the Vashishta and Singwi and Geldart and Taylor versions of the effective investigation.

The vertex function of the Hubbard approximation and those derived from the Vashishta and Singwi and Geldart and Taylor dielectric functions for  $r_s = 4.0$  are displayed in Fig. 2. Apart from a small deviation of the results of Vashishta and Singwi, the three all agree at  $q = 0$  because of the compressibility sum rule. They are all equal to unity at large  $q$ . The only difference among them is their  $q$  dependence in the intermediate region. We examine the two extremes—the Hubbard and Geldart and Taylor results—in detail in Sec. IV.

### III. CORE POLARIZATION IN REAL METALS

In a real metal there are additional contributions to the total dielectric function due to the response

of the periodic lattice of ions. The core electrons on each ion may polarize and the ions themselves may move in response to a charge perturbation. Here we consider only the former. In addition there are band-structure effects which we attempt to include by allowing an effective mass  $m_B$ . Taking the core polarizability to be a constant, we view the ionic background as a uniform, charged, and polarizable medium in which the electrons move. In order to generalize the effective electron-electron interaction to include the effects of core polarization, we must find the dielectric and vertex functions of the combined system of the electron gas and the polarizable background.

The importance of the dielectric medium has long been recognized in insulators and semiconductors,<sup>24,25</sup> where the background dielectric constant is large. The presence of the polarizable medium leads one to replace  $e^2$  by  $e^2/\epsilon_B$  in the theory of impurity states which results in energy levels that depend on  $1/\epsilon_B^2$  (Ref. 24) and an effective density of carriers determined by  $r_s/\epsilon_B$ . However, this effect has generally been ignored in metals where the dielectric constant is much smaller,  $\epsilon_B \sim 1-1.25$ .

We are led to reexamine the effects of core polarization because a treatment which considers only the conduction electrons predicts that the electron gas at densities corresponding to rubidium and cesium has a negative compressibility [Eq. (11)]. Others have considered the effects of core polarization in metals; Hedin<sup>26</sup> considered a model Hamiltonian and concluded that the properties of a metal should depend on  $r_s/\epsilon_B$  instead of  $r_s$ , and Perdew and Wilkins<sup>27</sup> presented a supporting plausibility argument. Vosko, Perdew, and MacDonald<sup>28</sup> have introduced crystalline and core electron effects into the density-functional theory of the spin susceptibility by treating the core electrons on the same footing as the conduction electrons. Our treatment is an extension of Hedin's.<sup>26</sup>

The total dielectric function of the combined system of electron gas and polarizable medium is given by

$$\epsilon(q) = \epsilon_B + V(q)\Pi(q, r_s, \epsilon_B, m_B). \quad (16)$$

Here  $\epsilon_B = 1 + 4\pi n\alpha$ , where  $\alpha$  is the ionic polarizability and  $n$  is the density of ions.  $\Pi$  is the electronic polarizability. We assume that  $\epsilon_B$  is unaffected by the presence of the electron gas. The goal is to calculate  $\Pi$  as a function of  $\epsilon_B$ .

The Hamiltonian for an electron gas with mass  $m_B$  immersed in a uniform background of dielectric constant  $\epsilon_B$  and perturbed by a charge  $ze$  at the origin is

$$H = \sum_i \frac{p_i^2}{2m_B} + \frac{e^2}{2\epsilon_B} \sum_{i \neq j} \frac{1}{|\hat{r}_i - \hat{r}_j|} - \frac{ze^2}{\epsilon_B} \sum_i \frac{1}{|\hat{r}_i|}. \quad (17)$$

We define a length scale by the density of electrons  $V/N = \frac{4}{3}\pi(r_s a_0)^3$  and measure lengths in units of  $r_s a_0$ , momenta in units of  $\hbar/(r_s a_0)$ , and energy in units of  $E_0 = \hbar^2/[m_B(r_s a_0)^2]$ . In terms of the dimensionless variables  $x = r/(r_s a_0)$ ,  $k = p/(r_s a_0)$ , and  $U = E/E_0$ , the Schrödinger equation becomes

$$\left[ \sum_i \frac{k_i^2}{2} + \frac{m_B e^2 r_s}{m \epsilon_B} \left( \frac{1}{2} \sum_{i \neq j} \frac{1}{|\hat{x}_i - \hat{x}_j|} - z \sum_i \frac{1}{|\hat{x}_i|} \right) \right] \Psi_D = U \Psi_D, \quad (18)$$

which only depends on the single parameter ( $m_B e^2 r_s / m \epsilon_B$ ) that measures the relative strength of the kinetic and potential-energy terms.

Since there is only one parameter in the theory, the solution of the problem of an electron gas with mass  $m_B$  and density determined by  $r_s$  immersed in a background with dielectric constant  $\epsilon_B$  is obtained by a simple scaling of the *known* solutions for an electron gas with mass  $m$  in a nonpolarizable background but at a different density determined by

$$r_s^* = m_B r_s / m \epsilon_B. \quad (19)$$

We show in Appendix A that the polarization scales as

$$\Pi(q, r_s, \epsilon_B, m_B) = [(m_B/m)^2 / \epsilon_B] \times \Pi(\epsilon_B m / m_B q, r_s^*, 1, m), \quad (20)$$

which must satisfy the modified compressibility sum rule

$$\frac{\Pi(0, r_s, \epsilon_B, m_B)}{\Pi^0(0, r_s, \epsilon_B, m_B)} = \frac{\Pi(0, r_s^*, 1, m)}{\Pi^0(0, r_s^*, 1, m)} = [\kappa/\kappa_0]_{r_s^*}, \quad (21)$$

where one replaces  $r_s$  by  $r_s^*$  in the compressibility ratio [Eq. (11)]. Identifying  $\Pi/\Pi^0$  with the vertex function [Eq. (15)], we see that the vertex function scales as

$$z(k_F, r_s, \epsilon_B, m_B) \Lambda(k_F, q, r_s, \epsilon_B, m_B) = z \left( \frac{m \epsilon_B}{m_B} k_F, r_s^*, 1, m \right) \times \Lambda \left( \frac{m \epsilon_B}{m_B} k_F, \frac{m \epsilon_B}{m_B} q, r_s^*, 1, m \right). \quad (22)$$

With these results we are in a position to completely specify our approximation of the effective electron-electron quasiparticle interaction in an electron gas immersed in a polarizable medium.

TABLE I. Ionic polarizabilities of the alkali metals.

Element	$r_s$	$\alpha(10^{-24} \text{ cm}^3)$	$\epsilon_B$	$r_s/\epsilon_B$
Li	3.25	0.025	1.015	3.20
Na	3.93	0.17	1.057	3.72
K	4.86	0.80	1.141	4.26
Rb	5.20	1.5	1.217	4.27
Cs	5.63	2.35	1.269	4.44

The semiempirical ionic polarizabilities of the alkali metals determined by Mayer and Mayer<sup>29</sup> are used to determine  $\epsilon_B$ . These values are in reasonably good agreement with the results of Pauling<sup>30</sup> and Dalgarno.<sup>31</sup> We list these polarizabilities together with  $\epsilon_B$  and  $r_s/\epsilon_B$  in Table I. We take  $m_B = 1$ .

Since the small  $q$  limit of the effective interaction is determined by the compressibility

$$U_{ee}(q=0) = \frac{4\pi}{q_{\text{TF}}^2} [\kappa/\kappa_0]_{r_s^*} \quad (23)$$

the most important consequence of including the effect of core polarization is to modify the compressibility ratio. Roughly speaking, the compressibility ratio [Eq. (11)] is given by

$$\kappa/\kappa_0 = \frac{1}{1 - r_s/5.18}, \quad (24)$$

which is modified to become

$$[\kappa/\kappa_0]_{r_s^*} = \frac{1}{1 - (r_s/\epsilon_B)/5.18}. \quad (25)$$

First we note that the criterion for a positive compressibility becomes  $r_s/\epsilon_B < 5.18$  rather than  $r_s < 5.18$ , and using the values of  $r_s/\epsilon_B$  from Table I, we see that rubidium and cesium are both renormalized into the region of positive compressibility. Furthermore, the strength of effective interaction at  $q=0$  depends strongly on  $\epsilon_B$ . For example, the small  $q$  limit of  $U_{ee}(q)$  in potassium is reduced by a factor of 3 by changing  $\epsilon_B$  from 1.0 to 1.14. This has a dramatic effect on the thermal resistivity which we calculate in Sec. IV.

#### IV. RESULTS AND CONCLUSIONS

##### A. Effective interaction in momentum space

We have calculated the effective interaction  $U_{ee}(q)$  [Eqs. (5), (8), and (15)] for various metals; typical results are displayed in Fig. 3. In Fig. 3(a) we plot  $U_{ee}(q)$  for  $r_s = 3.93$ , appropriate to sodium, and with a dielectric constant ( $\epsilon_B = 1.0$ ) which ignores core-polarization effects. The top curve (GT) gives  $U_{ee}(q)$  obtained from the Geldart and Taylor dielectric function; the middle curve (H) shows the result of the Hubbard approximation,

and the bottom curve, (TF) represents the Thomas-Fermi interaction. Figure 3(b) presents the same curves for sodium when the dielectric constant of the background is included. The same information for potassium,  $r_s = 4.86$ , is given in Figs. 3(c) and 3(d).

Consider first Figs. 3(a) and 3(b). All three curves in each agree at large  $q$ , because they go as  $1/\epsilon_B q^2$ . For intermediate  $q$  the Geldart and Taylor interaction is largest and has a definite shoulder where the slope is changing rapidly near  $q = 2k_F$ . The differences become more pronounced as we approach small  $q$ . The Hubbard and Geldart and Taylor interactions agree at  $q=0$  and are both much larger than the Thomas-Fermi result: this is because the Hubbard and Geldart and Taylor interactions both satisfy the compressibility sum rule, which the Thomas-Fermi result does not. This is the major failing of the Thomas-Fermi interaction. It is obvious from Fig. 3 that the only difference between the Hubbard and Geldart and Taylor interactions is their  $q$  dependence in the region from  $q=0$  to  $3k_F$ . Comparing Fig. 3(a) to 3(b) we see that the effect of including core polarization is to renormalize the  $q=0$  interaction, making it weaker [see discussion around Eq. (23)]. This is about a 10% effect in sodium.

The same general observations hold for the effective interaction in potassium, shown in Figs. 3(c) and 3(d), but the interaction is much stronger than in sodium and the effect of the polarizable background is much more dramatic.

In summary, Fig. 3 illustrates the two main points of this paper. *First*, the effective interaction is stronger than the Thomas-Fermi interaction for small  $q$ , and the discrepancy increases with increasing  $r_s$ . Since Eqs. (23) show that

$$\frac{U_{ee}(q=0)}{U_{\text{TF}}(q=0)} = [\kappa/\kappa_0]_{r_s^*} \approx \frac{1}{1 - (r_s/\epsilon_B)/5.18}, \quad (26)$$

we see that this effect is entirely due to the compressibility sum rule. *Second*, we emphasize the importance of  $\epsilon_B$  in the effective interaction in potassium. This is because  $\kappa/\kappa_0$  is a very sensitive function of  $r_s$  for  $r_s$  near 5.18 and the change from  $r_s$  to  $r_s/\epsilon_B$  results in a large decrease in the strength of the interaction.

##### B. Effective interaction in real space

The real-space potential is obtained by numerically Fourier transforming  $U_{ee}(q)$ ; the results for sodium and cesium are presented in Figs. 4(a) and 4(b). The curve (GT) shows the Geldart and Taylor interaction, the curve (H) gives the results of the Hubbard approximation, and the curve (TF) presents the Thomas-Fermi interaction.

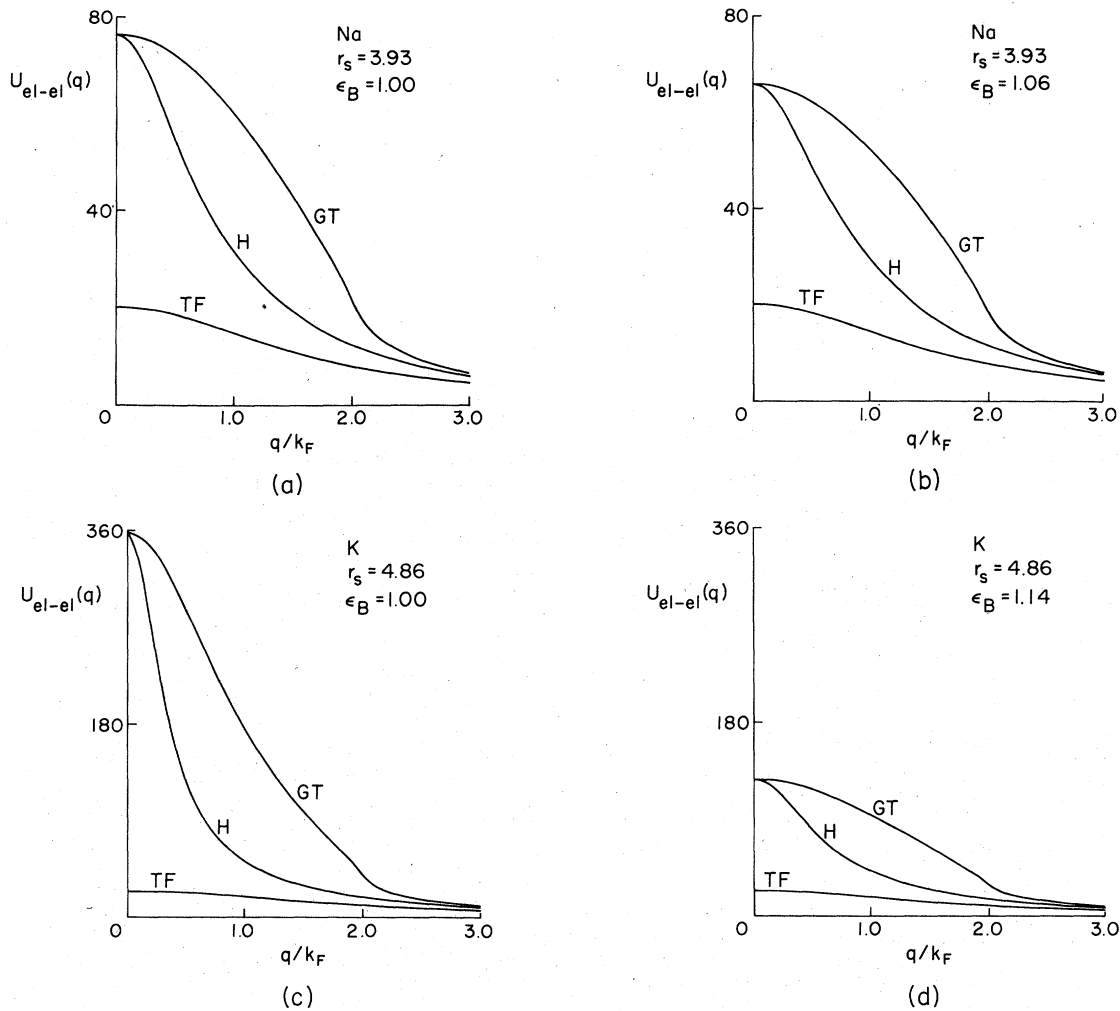


FIG. 3. Plot of the effective electron-electron interaction  $U_{ee}(q)$  in sodium [(a) and (b)] and potassium [(c) and (d)] as a function of  $q/k_F$ . The curves (GT) give the results obtained using the Geldart and Taylor dielectric function; the curves (H) show the results of the Hubbard approximation, and the curves (TF) represent the Thomas-Fermi screened Coulomb interaction. The dielectric constant due to core polarization is  $\epsilon_B$  and the  $\epsilon_B=1.00$  results are included for comparison. The potential is given in units of  $a_0^3(e^2/a_0)$ .

Several features of the curves in Fig. 4 deserve discussion. For small  $r$  ( $r \ll 1$ , which is not shown), all the potentials go as  $1/\epsilon_B r$ . This result, which arises from our model, is partially reasonable and partially not. Since the screening by conduction electrons is ineffective at short distances, the  $1/r$  behavior is expected. Similarly, the ion cores should not be effective in screening the interaction of two electrons for separations small compared to the lattice spacing, so we do not expect the  $1/\epsilon_B$  factor. However, our model, which takes  $\epsilon_B$  as independent of wave vector, *does* predict this factor. What rescues us is the fact that for small  $r$  the potential is so large (whether it is  $1/\epsilon_B r$  or  $1/r$ ) that electrons having energies

considered in this paper are classically forbidden to be in this region. Specifically, the phase shifts used in the transport calculations are insensitive to the form of the potential for  $r$  less than the classical turning point, set by condition  $U_{ee}(r)/\epsilon_F \sim 1$ . From Fig. 4 we see that the turning point is roughly at  $r=r_s$ , about a lattice spacing, so the particle never samples the small  $r$  region and any discrepancy in the potential for small  $r$  is irrelevant.

For intermediate  $r$  the Hubbard and Geldart and Taylor interactions have much harder cores than the Thomas-Fermi result, and since this is a classically allowed region we expect them to be stronger scatterers.



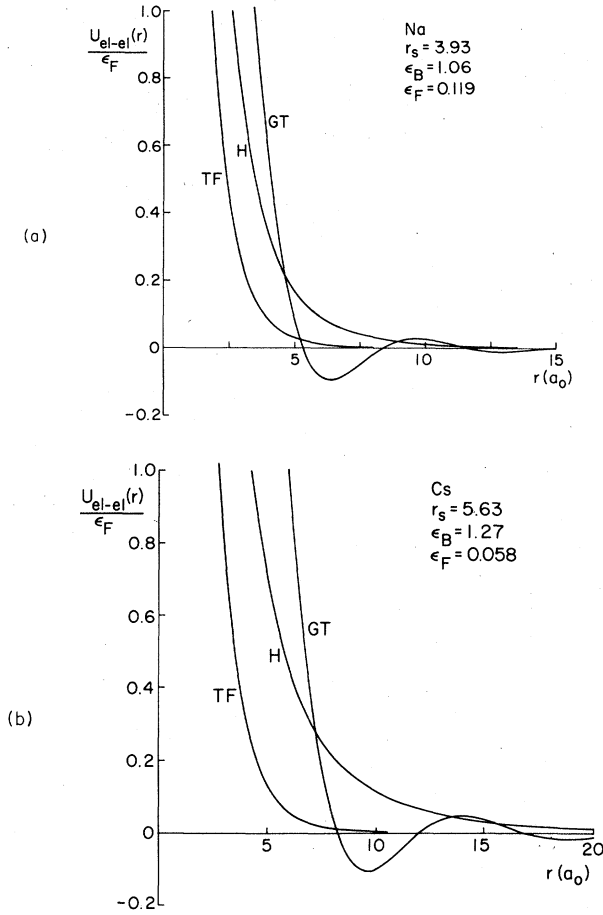


FIG. 4. (a) Plot of the effective electron-electron interaction  $U_{ee}(r)$ , measured in units of the Fermi energy, for sodium vs  $r$ . The curve (GT) gives the result obtained using the Geldart and Taylor dielectric function; the curve (H) shows the result of the Hubbard approximation, and the curve (TF) represents the Thomas-Fermi screened Coulomb interaction. (b) Same plot for cesium. Note the change in horizontal scale.

For somewhat larger  $r$  the Geldart and Taylor interaction oscillates and has shallow attractive regions which are due to Friedel oscillations.<sup>32</sup> These oscillations also appear in the Hubbard interaction, but the first zero is off the scale of the figure and their amplitude is extremely small.

Comparing Figs. 4(a) and 4(b) we see that the effective interaction is much stronger in cesium than in sodium.

### C. Interpolation formula for the effective interaction

The form of the Thomas-Fermi interaction [Eq. (2)] is familiar and relatively simple. It has been used extensively in calculations because it is the simplest screened interaction and it often permits

analytic solutions (e.g., transport coefficients calculated in the Born approximation). In order to try to take advantage of this simplicity we have constructed an interpolation formula for  $U_{ee}(q)$  in the Thomas-Fermi form that is consistent with both the compressibility sum rule and the large  $q$  limit,  $U_{ee}(q) \rightarrow 4\pi e^2 / \epsilon_B q^2$  formula,

$$U_{ee}^{int}(q) = \frac{4\pi e^2}{\epsilon_B(q^2 + q_s^2)}, \quad (27)$$

where

$$q_s^2 = \frac{q_{TF}^2}{\epsilon_B} [\kappa/\kappa_0] r_s^* \quad (28)$$

is exact in both these limits. This formula can be Fourier transformed analytically to yield

$$U_{ee}^{int}(r) = \frac{e^{-q_s r}}{\epsilon_B r}. \quad (29)$$

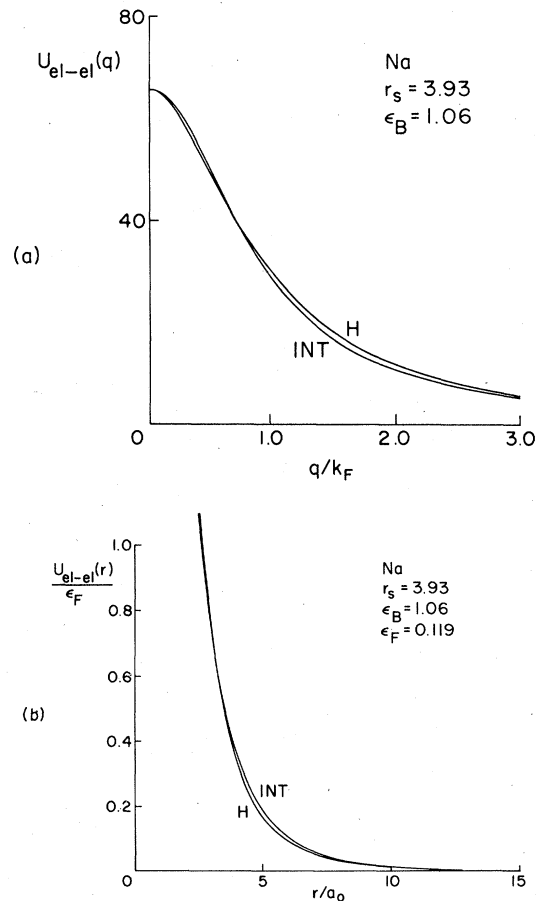


FIG. 5. Comparison of the interpolation formula (int) for the effective electron-electron interaction with the Hubbard interaction (H). (a) shows the comparison in momentum space, while (b) gives the real-space result.

The momentum and real-space versions of the interpolation formula are compared with the Hubbard interaction in Fig. 5, where we see that it is a close approximation to the more complicated Hubbard result. This is also evident from Table III in the next section where we exhibit the thermal resistivity calculated using the interpolation formula.

#### D. Thermal resistivity

The Boltzmann equation of the Fermi liquid with particle-particle scattering as the relaxation mechanism has been solved exactly, and the transport coefficients are determined by two angular averages of the phenomenological scattering rate.<sup>33</sup> In particular, the thermal resistivity is given by

$$W = (3/C_v V_F^2)(2\pi^2/3K\tau_0), \quad (30)$$

where  $C_v$  is the specific heat,  $V_F$  is the Fermi velocity, and  $\tau_0$  and  $K$  are related to angular averages of the scattering rate. Specifically, the relaxation time for a quasiparticle at the Fermi surface is  $2\tau_0/\pi^2$ , where  $1/\tau_0$  is proportional to an angular average of the scattering rate,

$$\frac{1}{\tau_0} = \frac{m^3 (k_B T)^2}{8\pi^4 \hbar^6} \langle \omega(k_1, k_2; k_1 + q, k_2 - q) \rangle. \quad (31)$$

$K$  depends weakly on another average of the scattering rate and, for the cases considered in this paper, we find that  $K$  is approximately constant and equal to 0.8. (The precise definitions of these averages are given in Refs. 3 and 33.) The point we wish to emphasize is that there is an exact prescription for obtaining the thermal resistivity due to electron-electron scattering once the quasiparticle scattering rate is known. Thus we can test our calculations of the scattering rate against experiment.

The scattering rate needed in Eq. (31) is the rate for the scattering of two quasiparticles from the states  $k_1$  and  $k_2$ , both on the Fermi surface, to states  $k_1 + q$  and  $k_2 - q$ , also on the Fermi surface. The lowest-order golden rule or Born approximation to this rate is obtained by considering a single scattering of the two particles via the effective interaction  $U_{ee}(q)$ . The total scattering rate can then be obtained, in principle, by summing all repeated particle-particle scatterings; in practice this means solving the Bethe-Salpeter equation for electron-electron scattering in a system at metallic density. To our knowledge this has not been done and obtaining such an exact solution is far beyond the scope of this paper. The Bethe-Salpeter equation is discussed in Appendix B, where it is pointed out that the main difficulty with its solution lies in the fact that the Pauli principle

restricts the available intermediate states to those unoccupied by other particles.

However, when the effective interaction is so simple as to depend only on a single momentum transfer, the problem of the scattering of the two free particles can be solved exactly by phase-shift analysis. We approximate the actual scattering rate by the free-particle rate. In Appendix B we argue that this is better than the Born approximation and show that the free-particle rate is self-consistent in that it reproduces the value of the compressibility built into the calculation via the compressibility sum rule.

Since our effective interaction depends only on  $q$ , the problem of the scattering of two free particles via this interaction can be reduced to a one-body problem in the center of mass of the particles.<sup>34</sup> The phase shifts are obtained by numerically solving the Schrödinger equation for a single particle in the effective potential  $U_{ee}(r)$ .

Within this scheme, the total scattering rate is related to the center-of-mass scattering cross section by<sup>3</sup>

$$\omega(k_1, k_2; k_1 + q, k_2 - q) = \frac{2\pi}{\hbar} \left( \frac{2\pi\hbar^2}{\mu} \right) \frac{\sigma(\theta)}{2}, \quad (32)$$

where  $\theta$  is the center-of-mass scattering angle,  $q = 2|\vec{k}_2 - \vec{k}_1| \sin(\frac{1}{2}\theta)$ , and  $\mu$  is the reduced mass, which is  $\frac{1}{2}m$  in this case. To obtain the transport coefficients we need to average over  $\theta$  and the relative energy,  $\epsilon = \frac{1}{2}|\vec{k}_2 - \vec{k}_1|^2/\mu$ , which ranges from 0 to  $2\epsilon_F$ . Using the standard phase shift expression for  $\sigma(\theta)$ <sup>35</sup> and taking the appropriate average over  $\theta$ , one finds that the thermal resistivity is given by<sup>3</sup>

$$W = \frac{16}{3} \frac{m^2 a_0^3 \gamma_s^3}{\hbar^3} \left( \frac{a_0^2}{4\pi K} \int_0^1 \frac{d\epsilon}{2\epsilon_F} \frac{\Sigma(\epsilon)}{[1 - (\epsilon/2\epsilon_F)]^{1/2}} \right) T, \quad (33)$$

where

$$\Sigma(\epsilon) = \sigma_0 + \frac{9}{2}\sigma_1 + \frac{55}{32}\sigma_2 + (10\pi/\epsilon) \sin\delta_0 \sin\delta_2 \sin(\delta_0 - \delta_2), \quad (34)$$

and

$$\sigma_l(\epsilon) = (4\pi/2\mu\epsilon)(2l+1) \sin^2\delta_l(\epsilon). \quad (35)$$

We have assumed (and verified by direct calculation) that all phase shifts beyond  $\delta_2$  are negligible.

What we have demonstrated in this section is that once we have an effective interaction that is so simple as to depend only on  $q$ , we can calculate an approximation to the scattering rate by phase-shift analysis. Given this approximate scattering rate, the thermal resistivity can be calculated exactly.

It should be remembered that the scattering rate

we have been discussing is the phenomenological rate that appears in the collision integral of the standard Boltzmann equation, and that our use of microscopic theory to form the scattering rate has been based on intuition. The Boltzmann equation for the Fermi liquid is itself a phenomenological equation, written down by Landau<sup>36</sup> for <sup>3</sup>He and generalized to the electron gas by Silin.<sup>37</sup> Eliashberg has derived the transport equation for a Fermi liquid from microscopic theory<sup>38</sup>; however, the equation he presents is of an unfamiliar form and cannot be compared directly with the Boltzmann equation. We have shown that the standard Boltzmann equation can be cast into the same form as Eliashberg's result.<sup>39</sup> Equating the two, we obtain a formula for the phenomenological scattering rate in terms of the four-point scattering function of many-body theory.

$$\omega(\vec{p}_1\vec{p}_2;\vec{p}'_1\vec{p}'_2) = \frac{2\pi}{\hbar} |z^2(p_F)\Gamma(\vec{p}_1, \vec{p}_2; \vec{p}'_1, \vec{p}'_2)|^2. \quad (36)$$

We examine the four-point scattering function in Appendix B and show how the form of the effective interaction may be motivated. We also see that there are other contributions to the scattering rate that are not included in our treatment of repeated particle-particle scattering via the effective interaction. The most obvious is repeated particle-hole scattering which we discuss briefly in Appendix B.

#### E. Numerical results

In order to directly compare the Hubbard and Geldart and Taylor interactions we have calculated the scattering cross sections [Eq. (35)] and the quantity  $\Sigma(\epsilon)$  needed for the thermal resistivity [Eq. (33)] for both these potentials. We list these quantities for sodium in Table II.

The trends shown in Table II may be roughly understood on the basis of the following considerations. For low incident energy the scattering samples the interaction only at large separations, where  $\epsilon > U_{\infty}(\nu)$  [Fig. 4(a)]. In this region the Hubbard interaction is stronger and we see that

the Hubbard total cross section is larger. For high incident energy,  $\epsilon_{\max} = 2\epsilon_F$ , the scattering samples the hard core of the interaction as well. Here the Geldart and Taylor interaction is larger, and we find that the Geldart and Taylor total cross section is also larger. The thermal resistivity is a weighted average of  $\Sigma(\epsilon)$  [Eq. (33)] that weights high energies most. The Hubbard  $\Sigma(\epsilon)$  is larger than that of Geldart and Taylor for all  $\epsilon$ , but they are quite close at  $\epsilon = 2\epsilon_F$ , so we expect the Hubbard resistivity to be close to the Geldart and Taylor result, but slightly larger.

We have calculated  $W$ , the thermal resistivity due to electron-electron scattering, for electron densities appropriate to aluminum, copper, and gold, as well as for the alkali metals. Although our analysis is valid only for free-electron-like metals such as the alkalis, we have included the others to show the  $\nu_s$  dependence of the theory. In Table III we compare the Hubbard and Geldart and Taylor predictions with each other and with experiment. We also list the results obtained using the Thomas-Fermi interaction and the interpolation formula [Eq. (29)].

From Table III we see that all the resistivities increase with  $\nu_s$ , and the Hubbard results are all somewhat larger than those of Geldart and Taylor, while both are much larger than the predictions of the Thomas-Fermi theory. We note that the predictions of the interpolation formula [Eq. (29)] are within 15% of the Hubbard resistivities.

We also list the same approximations for the scattering rate  $1/\tau$  in Table IV.  $\tau$  is the lifetime of an electron on the Fermi surface and our definition is related to that in Refs. 33 and 43 by  $\tau = (2/\pi^2)\tau_0$ . The scattering rates obtained in Ref. 43 to calculate the electrical resistivity were calculated using the Thomas-Fermi interaction.

The only element for which we can directly compare theory and experiment is sodium, where the measured value is  $W/T = 140 \pm 70 \times 10^{-6} \text{ cm}/W$ .<sup>1</sup> Both the Hubbard and Geldart and Taylor predictions fall within the experimental error, while the Thomas-Fermi results are a factor of 7 too

TABLE II. Scattering cross sections as a function of the incident energy for electron-electron scattering in sodium,  $\nu_s = 3.93$ ,  $\epsilon_B = 1.06$ . The symbols used are defined in the text [Eqs. (34) and (35)]. The total cross section including exchange is  $\sigma = \sigma_0 + 3\sigma_1 + \sigma_2$ .

Incident energy	Cross sections (in units of $a_0^3$ )									
	Hubbard					Geldart and Taylor				
$\epsilon/2\epsilon_F$	$\sigma_0$	$\sigma_1$	$\sigma_2$	$\sigma$	$\Sigma$	$\sigma_0$	$\sigma_1$	$\sigma_2$	$\sigma$	$\Sigma$
0.005	27.3	0	0	27.3	27.3	13.3	0	0	13.3	13.3
0.25	14.3	1.7	0.1	19.5	23.5	11.7	0.2	0	12.3	12.5
0.5	10.0	2.2	0.3	16.9	22.2	10.9	0.5	0	12.4	13.4
1.0	6.3	2.3	0.5	13.7	19.1	9.6	1.7	0	14.7	17.2

TABLE III. Electron-electron scattering contribution to the thermal resistivity. We compare various theoretical calculations with the experimental results of Cook and Laubitz *et al.* (Refs. 1, 2, and 40). The Thomas-Fermi results are obtained from the interpolation formula given in Ref. 3. The theoretical predictions for Al, Cu, and Au are free-electron results at the appropriate electron densities with  $\epsilon_B = 1$ . They are included simply to show the  $r_s$  dependence of the theories.

	$W/T$ ( $10^{-6}$ cm/W)							
	Al	Cu	Au	Li	Na	K	Rb	Cs
$r_s$	2.07	2.67	3.01	3.25	3.93	4.86	5.20	5.63
$\epsilon_B$	1	1	1	1.01	1.06	1.14	1.22	1.27
Experiment	0	4.4	7.3	...	$140 \pm 70$	$190^a$	$350^a$	$870^a$
Geldart and Taylor	1.9	8.3	17	28	95	460	660	1300
Hubbard	1.9	9.0	20	33	130	650	930	1800
Interpolation formula [Eq. (29)]	1.7	8.7	20	33	130	740	1100	2100
Thomas-Fermi	0.80	2.9	5.3	7.8	20	59	84	130

<sup>a</sup> These results became available after this paper was completed. We include them in this table, but they are not discussed in the text. The values for K and Cs are reported as preliminary. See Ref. 41.

small.<sup>42</sup> The Hubbard and Geldart and Taylor resistivities are close to each other for small  $r_s$ , but differ substantially for cesium, and it may be possible to differentiate them through experiment.

We point out that for a detailed comparison with experiment one would have to take into account deviations from Matthiessen's rule due to interference effects among the several scattering mechanisms. The dominance of phonon scattering at the high temperatures at which the experiments were done would cause deviations from additivity which are about 25% of the calculated resistivity and have the same temperature dependence as  $W$ .<sup>44</sup> Thus one should increase the theoretical values by about 25% to compare with experiment.

In Appendix B we argue that the use of the phase-shift analysis overestimates the calculated thermal resistivity by 5%–10% in Al and by 20%–35% in Cs. Therefore it is likely that our results for  $W$

and  $1/\tau$  are somewhat too large.

To see the effects of the polarizable background we have calculated  $W$  for sodium and potassium with  $\epsilon_B = 1.0$ , and compare them in Table V with the results obtained using realistic values of  $\epsilon_B$ .

From Table V and Figs. 3 and 4, we see that the effect of the polarizable background is to decrease the strength of the interaction between the quasiparticles and thus decrease  $W$ . Although the effect is relatively small in sodium, it is much larger in potassium, and experiments on potassium might be able to detect if our way of treating the polarizable background is adequate.

#### F. Concluding remarks

We wish to emphasize that the effective interaction between two electron quasiparticles depends strongly on the vertex function, which in turn must

TABLE IV. Electron-electron scattering rate  $1/\tau$ .  $\tau$  is the lifetime of an electron on the Fermi surface. Our definition is related to that of Ref. 33 and 43 by  $\tau = (2/\pi^2)\tau_0$ . The approximate Thomas-Fermi results were obtained by interpolation.

	$1/\tau T^2$ ( $10^6$ sec $^{-1}$ K $^{-2}$ )							
	Al	Cu	Au	Li	Na	K	Rb	Cs
$r_s$	2.07	2.67	3.01	3.25	3.93	4.86	5.20	5.63
$\epsilon_B$	1	1	1	1.01	1.06	1.14	1.22	1.27
Geldart and Taylor	1.4	2.9	4.2	5.3	10.3	26.0	30.4	45.6
Hubbard	1.5	3.3	5.0	6.6	14.5	41.1	47.8	72.3
Interpolation formula	1.4	3.2	5.1	6.8	15.4	45.7	53.3	82.1
Thomas-Fermi	~0.5	1.1	~1.5	~1.5	2.4	~3.5	~4.0	~4.9

TABLE V. Comparison of electron-electron scattering contribution to the thermal resistivity with and without a polarizable background.

$r_s$	$\epsilon_B$	(W/T) ( $10^{-6}$ cm/W)	
		Geldart and Taylor	Hubbard
3.93	1.00	110	150
	1.06	95	130
4.86	1.00	2000	2100
	1.14	460	650

satisfy the compressibility sum rule, so that this sum rule is of paramount importance in the effective interaction. Both the Hubbard and Geldart and Taylor theories have an adjustable parameter which is chosen to satisfy the sum rule, and they predict resistivities that are similar. The only other dielectric function that satisfies the sum rule is that of Vashishta and Singwi.<sup>7</sup> The vertex function derived from their dielectric function lies between those of Hubbard and Geldart and Taylor (Fig. 2) and we expect the resistivity also to lie between those two. Other dielectric functions, such as those of Singwi *et al.*,<sup>22</sup> Toigo and Woodruff,<sup>45</sup> and Kleinman,<sup>11</sup> deviate significantly from the sum rule at metallic densities and are inadequate to calculate the effective electron-electron interaction.

In summary, we have used two existing calculations of the dielectric function of the electron gas in order to calculate the effective electron-electron interaction. We have taken into account the effect of the polarizable background of ions in a real metal in an approximate but reasonable way which produces significant changes in the effective interaction. We have shown that the vertex function and the effects of the polarizable background are important at metallic densities and cannot be ignored. We use the effective interaction to calculate an approximate scattering rate. Given this scattering rate we calculate exactly the electron-electron scattering contribution to the thermal resistivity, a quantity that can be measured and that can thus provide a check of our results. Our calculations agree with the single experimental point now available, and we make predictions for all the alkali metals.

In closing we remark that although we have treated the compressibility and the background dielectric constant as well-known quantities, they are, after all, calculated (or deduced) values that are simply the best available at the present time, and as we have seen, the results become increasingly sensitive to their precise value as  $r_s$  increases.

#### ACKNOWLEDGMENTS

We benefited from many useful discussions with Bengt I. Lundqvist. We thank Peter Garik for comments on our treatment of core polarization. This work was supported in part by the Materials Science Center at Cornell University under a grant from the NSF.

#### APPENDIX A: SCALING OF THE DIELECTRIC FUNCTION

The dimensionless Schrödinger equation for an electron gas immersed in a polarizable background is given by Eq. (18). The dimensionless wave function  $\Psi_D$  depends on the coupling parameter  $r_s^* = (m_B r_s / m \epsilon_B)$  and the dimensionless variables  $\{\tilde{r}_i\}$ . The dimensionless energy  $U$  depends only on  $r_s^*$ .

The electron gas problem defined by [Eq. (18)] with  $m_B = m$  and  $\epsilon_B = 1$  has been solved in various approximations for many different values of  $r_s$ , the linear measure of the electron density. This means effectively that Eq. (18) has also been solved for different values of the coupling parameter  $r_s^*$ . Since  $\Psi_D$  depends only on this parameter, we see that the dimensionless wave function for the system at density  $r_s$  with mass  $m_B$  immersed in a dielectric medium,  $e^2 \rightarrow e^2 / \epsilon_B$ , is identical to the dimensionless wave function for a system with mass  $m$  in vacuum, but at a new density,  $r_s \rightarrow r_s^*$ .

The actual real-space wave function  $\Psi$  depends on dimensioned variables and will be different for these two cases. The connection between  $\Psi$  and  $\Psi_D$  for a system at density  $r_s$ , with mass  $m_B$  and the dielectric constant  $\epsilon_B$ , is given by

$$\Psi(r_s, \epsilon_B, m_B, \{\tilde{r}_i\}) = \Psi_D(r_s^*, 1, m, \{\tilde{r}_i / r_s a_0\}). \quad (37)$$

The wave function for the system at density  $r_s^*$ , with mass  $m$  and  $\epsilon_B = 1$ , is

$$\Psi(r_s^*, 1, m, \{\tilde{r}_i\}) = \Psi_D(r_s^*, 1, m, \{\tilde{r}_i / r_s^* a_0\}). \quad (38)$$

Therefore the scaling of the wave functions is given by

$$\Psi(r_s, \epsilon_B, m_B, \{\tilde{r}_i\}) = \frac{1}{[m \epsilon_B / m_B]^{3N/2}} \Psi(r_s^*, 1, m, \{(m_B / m \epsilon_B) \tilde{r}_i\}), \quad (39)$$

where the prefactor is a normalization constant. The dimensionless energies of the two systems are equal but in dimensioned units,

$$E(r_s, \epsilon_B, m_B) = (m_B / m) \frac{E(r_s^*, 1, m)}{\epsilon_B}. \quad (40)$$

Now that we have deduced the scaling of the wave functions we can calculate the scaling of the dielectric function by the standard derivation.

The change in the density induced by the static test charge density,  $\rho_{\text{ext}}(\vec{r}) = ze n_{\text{ext}}(\vec{r})$ , is given by<sup>46</sup>

$$\delta\langle n(\vec{r}) \rangle \equiv \langle n(\vec{r}) \rangle_H - \langle n(\vec{r}) \rangle_{H_0}, \quad (41)$$

where  $\langle \rangle_H$  denotes the expectation value calculated in the ground state of the full Hamiltonian, and  $H_0$  signifies the Hamiltonian of the electron gas in the absence of the test charge. Since the wave functions of  $H$  and  $H_0$  scale in the same way we need only consider one of them. We wish to express the induced density  $\delta\langle n(r, r_s, \epsilon_B, m_B) \rangle$  of a system at density  $r_s$  with mass  $m_B$  and with a dielectric background  $\epsilon_B$  in terms of the induced density  $\delta\langle n(r, r_s^*, 1, m) \rangle$  of a system with density  $r_s^*$  with

mass  $m$  and without a dielectric background. The expectation value of the density is given by

$$\langle n(\vec{r}, r_s, \epsilon_B, m_B) \rangle = \int \{d\vec{r}_i\} |\Psi(r_s, \epsilon_B, m_B, \{\vec{r}_i\})|^2 n(\vec{r}, \{\vec{r}_i\}), \quad (42)$$

where

$$n(\vec{r}, \{\vec{r}_i\}) = \sum_i \delta(\vec{r} - \vec{r}_i) = \left(\frac{m_B}{m\epsilon_B}\right)^3 n\left(\frac{m_B\vec{r}}{m\epsilon_B}, \left\{\frac{m_B\vec{r}_i}{m\epsilon_B}\right\}\right).$$

Using the simple scaling of the density operator and the scaling of the wave function, it is found that

$$\begin{aligned} \langle n(\vec{r}, r_s, \epsilon_B, m_B) \rangle &= \int \left\{ \frac{m_B d\vec{r}_i}{m\epsilon_B} \right\} \left| \Psi\left(r_s^*, 1, m, \left\{ \frac{m_B \vec{r}_i}{m\epsilon_B} \right\}\right) \right|^2 \left(\frac{m_B}{m\epsilon_B}\right)^3 n\left(\frac{m_B\vec{r}}{m\epsilon_B}, \left\{ \frac{m_B \vec{r}_i}{m\epsilon_B} \right\}\right) \\ &= \left(\frac{m_B}{m\epsilon_B}\right)^3 \left\langle n\left(\frac{m_B\vec{r}}{m\epsilon_B}, r_s^*, 1, m\right) \right\rangle. \end{aligned} \quad (43)$$

Fourier transforming, we have

$$\langle n(q, r_s, \epsilon_B, m_B) \rangle = \langle n[(m\epsilon_B/m_B)q, r_s^*, 1, m] \rangle. \quad (44)$$

The induced density scales in exactly the same way. Note that this is an exact scaling result and does not depend on a linear approximation, thus it must be preserved in all orders of perturbation theory.

In linear response theory the induced density is related to the polarization by

$$\delta\langle n(\vec{q}) \rangle = (-V\Pi/\epsilon)n_{\text{ext}}(\vec{q}). \quad (45)$$

For our own case  $n_{\text{ext}}(\vec{q}) = 1$  and using Eq. (16) we obtain the scaling of the polarization given in Eq. (20).

$$\delta\langle n(q) \rangle = -\frac{V[(m\epsilon_B/m_B)q]\Pi[(m\epsilon_B/m_B)q, r_s^*, 1, m]n_{\text{ext}}[(m\epsilon_B/m_B)q]}{1 + V[(m\epsilon_B/m_B)q]\Pi[(m\epsilon_B/m_B)q, r_s^*, 1, m]}. \quad (48)$$

Using Eqs. (46) and (47) and  $n_{\text{ext}}(\vec{q}) = 1$ , we obtain the final result

$$\epsilon(q) = \epsilon_B + \frac{V(q)}{\epsilon_B} \Pi\left(\frac{m\epsilon_B}{m_B}q, r_s^*, 1, m\right). \quad (49)$$

#### APPENDIX B: THE FOUR-POINT SCATTERING FUNCTION AND THE EFFECTIVE INTERACTION

In this Appendix we show that our use of the effective electron-electron interaction [Eq. (5)] to

Equivalently, we may use the definition of the dielectric function which yields the net electrostatic potential due to a perturbation by  $n_{\text{ext}}(\vec{q})$ ,

$$1/\epsilon = 1 + \delta n_{\text{total}}/n_{\text{ext}} \quad (46)$$

For our two component system  $\delta n_{\text{total}} = \delta\langle n(\vec{q}) \rangle + \delta n_{\text{back}}$ , where  $\delta n_{\text{back}}$  is the charge induced in the background of ions. The background responds to both  $n_{\text{ext}}$  and  $\delta\langle n(\vec{q}) \rangle$ ,

$$\delta n_{\text{back}} = (1/\epsilon_B - 1)(n_{\text{ext}} + \delta\langle n(q) \rangle). \quad (47)$$

The scaling argument shows that  $\delta\langle n(\vec{q}) \rangle$  is obtained by scaling the response of a system with  $\epsilon_B = 1$  and  $m_B = m$ ,

calculate the quasiparticle scattering rate [Eq. (31)] may be motivated by considering the exact expression for the scattering rate in terms of the four-point scattering function.

The four-point scattering or vertex function,  $\Gamma(1, 2, 1', 2')$ , is the transition amplitude for the process  $(1, 2) \rightarrow (1', 2')$ , where 1 stands for  $p_1\sigma_1$ .<sup>47</sup>  $\Gamma$  is the sum of all diagrams that can be connected to two incoming and two outgoing particle lines. It is convenient to separate  $\Gamma$  into an irreducible part and then consider repeated scatterings via

the irreducible interaction.<sup>48</sup> This procedure leads to the Bethe-Salpeter integral equation for  $\Gamma$ .

There are three ways to separate  $\Gamma$  into an irreducible part and repeated scatterings and thus there are three Bethe-Salpeter equations which are graphically represented in Fig. 6. The equation for repeated particle-particle scattering is given in Fig. 6(a); Fig. 6(b) shows the Bethe-Salpeter equation in one particle-hole channel; and Fig. 6(c) shows the other particle-hole channel.

Since we are interested in transport properties which depend on electron-electron scattering, the appropriate channel to work in is the particle-particle channel, so we need the irreducible interaction  $J$ . In order to form an approximation to  $J$  we note four points. First, the exact expression for  $J$  will be the sum of three classes of diagrams—those that are irreducible in all channels plus those that are reducible in one particle-hole channel plus those reducible in the other particle-hole channel. Second, if one chooses the irreducible interactions  $I$  and  $K$  of the particle-hole channels to be totally irreducible, then the approximations to  $\Gamma$  (designated by  $\Gamma_I$  and  $\Gamma_K$ ) obtained by solving the Bethe-Salpeter equations in the particle-hole channels will be irreducible in the particle-particle channel. Third, since the two particle-hole channels map into each other upon interchange of the incoming or outgoing particles we need only consider one of them. Fourth,  $\Gamma$  is a

scattering amplitude and must be antisymmetric under interchange of the incoming or outgoing particles. This means that  $J$  must also be antisymmetric.

Therefore, by choosing the irreducible particle-hole interaction to be totally irreducible (designated by  $\Delta$ ) and by choosing  $K=I$  and solving the resulting Bethe-Salpeter equations, we obtain an approximation for  $J_{\parallel}$ , the irreducible interaction between electrons with parallel spins:

$$J_{\parallel} = \Delta + (\Gamma_I - \Delta) - (\Gamma_K - \Delta), \tag{50}$$

which is both irreducible and antisymmetric when  $\Delta$  is antisymmetric. We consider scattering from states  $p_1, \sigma_1$  and  $p_2, \sigma_2$  to  $p_1+q, \sigma_1$  and  $p_2-q, \sigma_2$ , as in Fig. 6(b), and we choose the totally irreducible interaction to be

$$\Delta = V(q)\delta\sigma_1\sigma_1' \delta\sigma_2\sigma_2' - V(p_2-p_1-q)\delta\sigma_1\sigma_2 \delta\sigma_2\sigma_1'. \tag{51}$$

We iterate the Bethe-Salpeter equation and graphically represent the terms through third order in Fig. 7. Certain of these diagrams may be summed to infinite order and the resulting approximation  $\Gamma_I$  is shown in Fig. 8(a). The effective interaction between electrons with opposite spins is given by the first diagram in the expansion of  $\Gamma_I$  shown in Fig. 8(a). This has precisely the form of Eq. (5). We obtain  $\Gamma_K$  from  $\Gamma_I$  by interchanging 1' and 2'. We may now form  $J_{\parallel}$ , our approximation to the irreducible particle-particle interaction, which is shown in Fig. 8(a).

Our effective interaction approximation for  $J_{\parallel}$

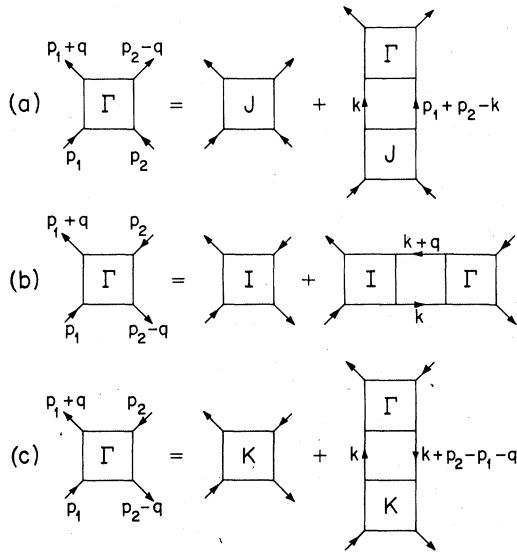


FIG. 6. Graphical representation of the Bethe-Salpeter equations for the four-point scattering function  $\Gamma$ . The particle-particle channel is shown in (a), and the two particle-hole channels are presented in (b) and (c).

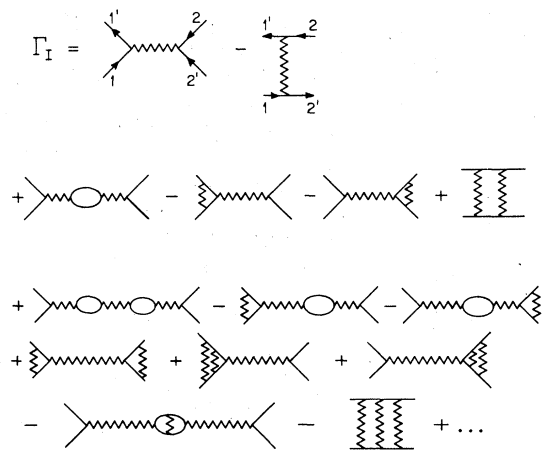


FIG. 7. Graphical representation of the iterative solution of the Bethe-Salpeter equation in the particle-hole channel of Fig. 6(b). The two first-order terms are the approximation to the irreducible interaction  $I$  [Eq. (51)], and the second- and third-order terms arise from repeated scatterings via the irreducible interaction.

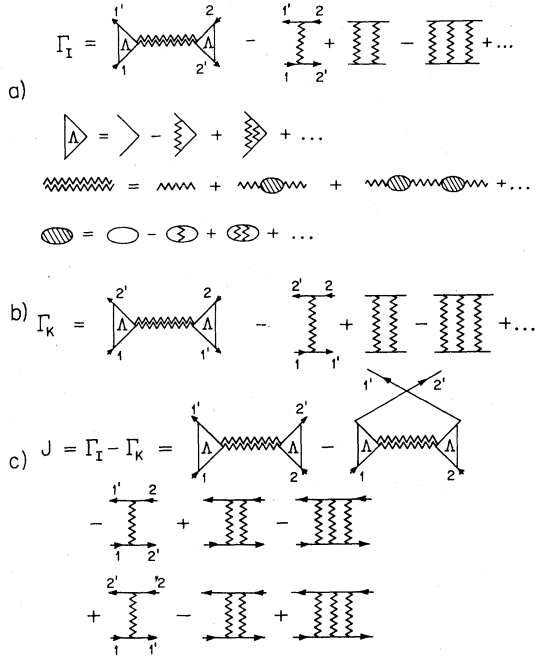


FIG. 8. Approximation of  $J$ , the irreducible interaction in the particle-particle channel of Fig. 6(a). The approximation is  $J_{\uparrow\uparrow} = \Delta + (\Gamma_I - \Delta) - (\Gamma_K - \Delta)$  [Eq. (50)], where  $\Delta$  is the totally irreducible interaction of Eq. (51) and  $\Gamma_I$  and  $\Gamma_K$  are solutions of the Bethe-Salpeter equation in the two particle-hole channels for the particular choice of irreducible interactions  $I=K=\Delta$ . We show in Fig. 8(a) the  $\Gamma_I$  obtained by summing certain of the diagrams of Fig. 7 to infinite order. The solution  $\Gamma_K$  in the other particle-hole channel is obtained from  $\Gamma_I$  by interchanging the outgoing particles. The resulting approximation for  $J_{\uparrow\uparrow}$  is given in (c). The irreducible interaction between electrons of antiparallel spins is given by the first diagram for  $\Gamma_I$  in (a).

includes the first two terms shown in Fig. 8(b) and ignores all other contributions. Stopping here at least results in a screened interaction which is consistent with our preconceptions. To get these first two terms we have summed up an infinite subset of all possible diagrams of  $J$ , but as is typical in diagram calculations an infinite number of diagrams are also omitted. One class of diagrams that are obviously neglected are those shown in Fig. 8(c). These diagrams represent repeated particle-hole scatterings and are important in calculations of the paramagnetic susceptibility in metals such as palladium that have a large susceptibility enhancement. However, it is believed that paramagnons—repeated particle-hole scatterings—are not important in the simple metals where the susceptibility enhancement is small. Our approximation of  $J$  already includes the first-order term and we neglect only the repeated scatterings. We expect this to be a reason-

able approximation in simple metals.

Now that we have the irreducible particle-particle interaction we must solve the Bethe-Salpeter equation [Fig. 6(a)] for the four-point scattering function  $\Gamma$ . Unfortunately, the Bethe-Salpeter equation for electron-electron scattering in the presence of the Fermi sea cannot be solved analytically for any realistic irreducible interaction and we know of no numerical solutions of the electron-electron problem (at metallic densities).

What is typically done when considering transport in metals is to use the Born approximation,

$$\Gamma_{\text{Born}} = J, \quad (52)$$

and ignore all repeated scatterings.<sup>2,48,49</sup>

Another approximation becomes possible when the irreducible interaction is so simple as to depend only on a single momentum transfer. The direct term of our approximation,  $J = U_{\infty}(q)$ , is a single screened interaction which satisfies the above condition. This simplification results in the ladder approximation to the Bethe-Salpeter equation<sup>50</sup> which can be solved exactly for free-particle scattering in the absence of the Fermi sea by a phase-shift analysis. The resulting free-particle scattering amplitude is denoted by  $f$  and the approximation for the four-point function is

$$\Gamma_{\text{free}} = 4\pi f. \quad (53)$$

In the presence of the filled Fermi sea, the actual scattering amplitude differs from  $f$  because the Pauli principle restricts the number of intermediate states to those unoccupied by other particles. Furthermore, a calculation of the actual scattering amplitude involves the full propagator of the interacting system, not simply the free-particle propagator. If one continues to use free-particle propagators, but wants to include the effect that the Fermi sea has in restricting the intermediate states, one obtains Galitskii's integral equation for  $\Gamma$ ,<sup>51,52</sup> which is symbolically represented as

$$\Gamma = 4\pi f + 4\pi f G_0^2 \Gamma. \quad (54)$$

Galitskii solved this equation approximately by iteration for a low density Fermion gas, but no results are available at metallic densities where the iterative method fails. Even if this equation were solved exactly it would yield only an approximate  $\Gamma$  calculated with free-particle propagators  $G_0$ .

Since an attempt to numerically solve the Bethe-Salpeter equation is beyond the scope of this paper, we are forced to use either the Born approximation or the free-particle phase-shift approximation of  $\Gamma$ . It is difficult to determine the validity of any approximation unless one knows the exact answer



to enable comparisons. However, we have certain prejudices for a repulsive interaction. It is well known that the Born approximation overestimates the scattering amplitude for free particles<sup>2,53</sup> because it does not take into account the fact that the scattering potential alters the particle's wave function. The same effect occurs in the presence of the Fermi sea, so we feel that the phase-shift amplitude is a better approximation to  $\Gamma$  than the Born approximation.

The forward scattering limit of the exact  $\Gamma$  determines the Fermi-liquid parameters because it is related to the Landau scattering function  $A(p_1, p_2)$  by<sup>54</sup>

$$z^2(k_F)\bar{\Gamma}(p_1\sigma_1, p_2\sigma_2; p_1\sigma'_1, p_2\sigma'_2) = A(p_1, p_2), \quad (55)$$

where the proper four-point function  $\bar{\Gamma}$  is given by

$$\bar{\Gamma} = \Gamma - \Lambda^2(k_F, q)V(q)/\epsilon(q). \quad (56)$$

The Fermi-liquid parameters may be obtained by the relations<sup>54,55</sup>

$$z^2(k_F)\bar{\Gamma}_{,,} + \bar{\Gamma}_{,,} = \frac{2}{\nu(0)} \sum_{l=0}^{\infty} \frac{A_l}{1 + A_l/2l + 1} P_l(\cos\theta), \quad (57)$$

and

$$z^2(k_F)(\bar{\Gamma}_{,,} - \bar{\Gamma}_{,,}) = \frac{2}{\nu(0)} \sum_{l=0}^{\infty} \frac{B_l}{1 + B_l/2l + 1} P_l(\cos\theta), \quad (58)$$

where  $\bar{\Gamma}_{,,} = \bar{\Gamma}(p_1\sigma, p_2\sigma; p_1\sigma, p_2\sigma)$  and  $\bar{\Gamma}_{,,} = \bar{\Gamma}(p_1\sigma, p_2 - \sigma; p_1\sigma, p_2 - \sigma)$  depend on the angle  $\theta$  between  $p_1$  and  $p_2$ ,  $\nu(0) = m_B p_F / \pi^2 \hbar^3$ .

The Fermi-liquid parameter  $A_0$  determines the compressibility<sup>56</sup> ( $\kappa_0/\kappa = 1 + A_0$  for  $m^*/m = 1$ ) so we can test the self-consistency of our approximations for  $\Gamma$  by using  $\Gamma$  to calculate  $A_0$  and comparing it with the value of  $A_0$  we have built into the dielectric and vertex functions through the compressibility sum rule. We can also calculate other

Fermi-liquid parameters and compare our predictions with the results of others.

The two approximations we want to test are the Born approximation and the modified phase-shift result  $\Gamma = 4\pi f$ . The Born approximation is entirely real so that the calculation of Landau parameters via the identification of Eq. (55) is straightforward. On the other hand, the phase-shift approximation for  $\Gamma$  is complex because  $f$  satisfies the optical theorem, and the identification of Eq. (55) is ambiguous. Nozieres<sup>57</sup> points out that the imaginary part of the exact  $\Gamma$  is proportional to the imaginary part of the self-energy which goes to zero for particles on the Fermi surface. At first sight the phase-shift approximation seems unsatisfactory because it has an imaginary part. However, if one examines Galitskii's solution of the integral equation [Eq. (54)] in the low density limit,<sup>58</sup> one sees that one effect of the first iteration is to exactly cancel the imaginary part of  $f$  so that to leading order in the low density limit,  $\Gamma = \text{Re} 4\pi f$ . We suspect that a similar cancellation also occurs at metallic densities. If  $\Gamma$  must be real, the approximation  $\Gamma = 4\pi f$  is ruled out, but the approximation

$$\Gamma = \text{Re} 4\pi f \quad (59)$$

is acceptable and would seem reasonable if the primary effect of solving the integral equation was simply to cancel the imaginary part of  $f$ .

The Fermi-liquid parameters  $A_0$  and  $B_0$  which determine the compressibility and susceptibility,<sup>56</sup> respectively, have been calculated using both the Born approximation and the modified phase-shift approximation of Eq. (59), and the results are displayed in Table VI, where they are compared with the values of  $A_0$  we have built into the calculation via the compressibility sum rule and with Hedin's<sup>59</sup> calculated values of  $B_0$ . The interpolation formula (which is a good approximation to the Hubbard interaction) predicts values of  $A_0$  which

TABLE VI. Test of the self-consistency of the approximations of the four-point scattering function  $\Gamma$ . The Fermi-liquid parameters  $A_0$  and  $B_0$  which determine the compressibility and the susceptibility are calculated from the approximations of  $\Gamma$  and the results are compared with the value of  $A_0$  built into the calculation via the compressibility sum rule and with Hedin's calculations of  $B_0$ .

		$A_0 = \kappa_0/\kappa - 1$			$A_0 = B_0$		$B_0 = \chi_0/\chi - 1$	
		Input	Interpolation formula	Geldart and Taylor	Born	Hedin	Interpolation formula	Geldart and Taylor
Al	$r_s = 2.07$							
	$\epsilon_B = 1.0$	-0.37	-0.39	-0.44	-0.23	-0.25	-0.18	-0.19
Cs	$r_s = 5.63$							
	$\epsilon_B = 1.27$	-0.84	-0.83	-0.86	-0.51	-0.32	-0.26	-0.15

are in excellent agreement with the input values. The Geldart and Taylor results also show good agreement. Even though we have ignored the contribution of repeated particle-hole scatterings to the susceptibility, both the interpolation formula and the Geldart and Taylor interaction predict values of  $B_0$  that are in fair agreement with the results of Hedin's calculations. On the other hand, the Born approximation predicts that  $A_0 = B_0$  and the numerical values are not in good agreement with either the input  $A_0$  or Hedin's  $B_0$ .

We feel that these results indicate that the approximation  $\Gamma = \text{Re } 4\pi f$  is better than the Born approximation and the degree of self-consistency suggests that it is close to the true  $\Gamma$ . In this paper, however, we have used  $\Gamma = 4\pi f$ , which is a more systematic approximation. If in fact a more correct identification is  $\Gamma = \text{Re } 4\pi f$ , then the physical quantities we have calculated which depend on various averages of

$$|\Gamma|^2 = (\text{Re } 4\pi f)^2 + (\text{Im } 4\pi f)^2 \quad (60)$$

would overestimate these quantities by roughly the ratio

$$|\Gamma|^2 / (\text{Re } 4\pi f)^2. \quad (61)$$

Direct calculations using  $\Gamma = \text{Re } 4\pi f$  show that the new values of the electron-electron scattering contribution to the thermal resistivity compared

to those in Table III would range from 5% smaller in Al using the interpolation formula and 12% in Al using the Geldart and Taylor interaction to 20% smaller in Cs using the interpolation formula and 35% in Cs using the Geldart and Taylor result.

In summary, we believe that we have included most of the essential physics in our choice of the irreducible particle-particle interaction  $J$ . Given  $J$ , we have made an approximation for  $\Gamma$  that appears to be reasonably self-consistent, but we have not solved the Bethe-Salpeter equation and a strict criterion for the validity of our approximation is not known.

{Note added: The terms of Fig. 8(c) beyond the first two, were neglected in forming the effective interaction between electrons with parallel spins. However, these terms may also be summed to infinite order in the spirit of the Hubbard approximation which assumes that each interaction line depends only on the momentum transferred between the external electrons. This yields a correction to  $J_{\uparrow\uparrow}$ , and to  $U_{\sigma\uparrow\sigma}$ , [Eq. (6)]:

$$\delta V_{\sigma\uparrow\sigma} = \delta J_{\uparrow\uparrow} = -[\Lambda(1-\Lambda-1)^2/\Pi^0]_q + [\Lambda(1-\Lambda-1)^2/\Pi^0]_{p_2-p_1-a}.$$

This correction term was first obtained by another method by Kukkonen and Overhauser (to be published). The effect of this term has not been investigated.}

\*Present address.

<sup>1</sup>J. G. Cook, M. P. Van der Meer, and M. J. Laubitz, *Can. J. Phys.* **50**, 1386 (1972).

<sup>2</sup>M. J. Laubitz, *Phys. Rev. B* **2**, 2252 (1970).

<sup>3</sup>C. A. Kukkonen and H. Smith, *Phys. Rev. B* **8**, 4601 (1973).

<sup>4</sup>J. Hubbard, *Proc. R. Soc. A* **243**, 336 (1957).

<sup>5</sup>D. J. W. Geldart and S. H. Vosko, *Can. J. Phys.* **44**, 2137 (1966).

<sup>6</sup>D. J. W. Geldart and R. Taylor, *Can. J. Phys.* **48**, 155, 167 (1970).

<sup>7</sup>P. Vashishta and K. S. Singwi, *Phys. Rev. B* **6**, 875 (1972); 883(E) (1972).

<sup>8</sup>J. Lindhard, *Kgl. Danske Videnskab. Selskab, Mat.-Fys. Medd.* **28**, 8 (1954).

<sup>9</sup>V. Heine, P. Nozières, and J. W. Wilkins, *Philos. Mag.* **13**, 741 (1966).

<sup>10</sup>M. Rasolt, *J. Phys. F* **5**, 2294 (1975).

<sup>11</sup>L. Kleinman, *Phys. Rev.* **172**, 383 (1968).

<sup>12</sup>L. Hedin and S. Lundqvist, *Solid State Phys.* **23**, 1 (1969).

<sup>13</sup>L. D. Landau, *Sov. Phys. JETP* **8**, 70 (1959).

<sup>14</sup>L. P. Pitayevski, *Sov. Phys. JETP* **10**, 1267 (1960).

<sup>15</sup>J. M. Luttinger and P. Nozières, *Phys. Rev.* **127**, 1423 (1962); **127**, 1431 (1962).

<sup>16</sup>P. Nozières, *Interacting Fermi Systems* (Benjamin, New York, 1964), p. 287.

<sup>17</sup>T. M. Rice, *Ann. Phys.* **31**, 100 (1965), Eq. (57).

<sup>18</sup>Reference 4, p. 103.

<sup>19</sup>L. Hedin and B. I. Lundqvist, *J. Phys. C* **4**, 2064 (1971).

<sup>20</sup>It is interesting that the Vashishta-Singwi compressibility agrees almost exactly with that obtained by differentiating the Nozières-Pines interpolation formula for the energy. N. W. Ashcroft and D. C. Langreth, *Phys. Rev.* **159**, 500 (1967).

<sup>21</sup>D. C. Langreth, *Phys. Rev.* **181**, 753 (1969). Langreth does include a parameter which allows to be fixed by the compressibility sum rule, but his dielectric function is very similar to the Hubbard approximation and we do not discuss it separately.

<sup>22</sup>K. S. Singwi, A. Sjölander, M. P. Tosi, and R. H. Land, *Phys. Rev. B* **1**, 1044 (1970).

<sup>23</sup>D. J. W. Geldart and R. Taylor, *Solid State Commun.* **9**, 7 (1971).

<sup>24</sup>W. Kohn, *Phys. Rev.* **105**, 509 (1957); **110**, 857 (1957).

<sup>25</sup>P. A. Wolff, *Phys. Rev.* **126**, 405 (1962).

<sup>26</sup>L. Hedin, *Ark. Fys.* **30**, 231 (1965).

<sup>27</sup>J. P. Perdew and J. W. Wilkins, *Phys. Rev. B* **7**, 2461 (1973).

<sup>28</sup>S. H. Vosko, J. P. Perdew and A. H. MacDonald, *Phys. Rev. Lett.* **35**, 1725 (1975).

<sup>29</sup>J. E. Mayer and M. G. Mayer, *Phys. Rev.* **43**, 605 (1933).

<sup>30</sup>L. Pauling, *Proc. R. Soc. A* **114**, 181 (1927).

- <sup>31</sup>A. Dalgarno, *Adv. Phys.* 11, 281 (1962).
- <sup>32</sup>A. L. Fetter and J. D. Walecka, *Quantum Theory of Many-Particle Systems* (McGraw-Hill, New York, 1971), p. 179.
- <sup>33</sup>H. Højgaard-Jensen, H. Smith, and J. W. Wilkins, *Phys. Rev.* 185, 323 (1969); *Phys. Lett.* 27A, 532 (1968).
- <sup>34</sup>L. I. Schiff, *Quantum Mechanics*, 3rd ed. (McGraw-Hill, New York, 1968), p. 116.
- <sup>35</sup>Reference 34, p. 374.
- <sup>36</sup>L. D. Landau, *Sov. Phys. JETP* 3, 920 (1956).
- <sup>37</sup>V. P. Silin, *Sov. Phys. JETP* 6, 387 (1957); 6, 985 (1957).
- <sup>38</sup>G. M. Eliashberg, *Sov. Phys. JETP* 14, 408 (1962).
- <sup>39</sup>Carl A. Kukkonen, Ph.D. thesis (Cornell University, 1975) (unpublished).
- <sup>40</sup>M. J. Laubitz and J. G. Cook, *Phys. Rev. B* 6, 2082 (1972); 7, 2867 (1973).
- <sup>41</sup>J. G. Cook and M. J. Laubitz, in *Thermal Conductivity 14*, edited by P. G. Klemens and T. K. Chu (Plenum, New York, 1976); J. G. Cook (unpublished).
- <sup>42</sup>In our calculations we have used low-temperature values of  $r_s$ , while the experiments are done at high temperature. The correct values of  $r_s$  to use for comparison are about 1% or 2% larger than the values we use; however, this discrepancy does not affect our results significantly.
- <sup>43</sup>W. E. Lawrence and J. W. Wilkins, *Phys. Rev. B* 7, 2317 (1973).
- <sup>44</sup>H. Smith and J. W. Wilkins, *Phys. Rev.* 183, 624 (1969).
- <sup>45</sup>F. Toigo and T. O. Woodruff, *Phys. Rev. B* 2, 3958 (1970).
- <sup>46</sup>Reference 32, p. 172.
- <sup>47</sup>P. Nozières, *Interacting Fermi Systems* (Benjamin, New York, 1964), p. 105.
- <sup>48</sup>Reference 47, p. 239.
- <sup>49</sup>See References 1-4 cited in Ref. 3.
- <sup>50</sup>Reference 32, p. 137.
- <sup>51</sup>V. M. Galitskii, *Sov. Phys. JETP* 7, 104 (1958).
- <sup>52</sup>Reference 32, p. 141.
- <sup>53</sup>E. Abrahams, *Phys. Rev.* 95, 839 (1954).
- <sup>54</sup>Reference 47, pp. 264 and 286.
- <sup>55</sup>K. S. Dy and C. J. Pethick, *Phys. Rev.* 185, 373 (1969).
- <sup>56</sup>T. M. Rice, *Phys. Rev.* 175, 858 (1968).
- <sup>57</sup>Reference 47, pp. 292 and 109.
- <sup>58</sup>Reference 32, p. 143.
- <sup>59</sup>L. Hedin, *Phys. Rev.* 139, A796 (1965).